Estimating Atterberg limits of soils from hygroscopic water content

Arthur, Emmanuel; Rehman, Hafeez Ur; Tuller, Markus; Pouladi, Nastaran; Nørgaard, Trine; Moldrup, Per; de Jonge, Lis Wollesen

Published in:
Geoderma

DOI (link to publication from Publisher):
10.1016/j.geoderma.2020.114698

Publication date:
2021

Document Version
Publisher's PDF, also known as Version of record

Geoderma 381 (2021) 114698

Contents lists available at ScienceDirect

Geoderma

journal homepage: www.elsevier.com/locate/geoderma

Estimating Atterberg limits of soils from hygroscopic water content

Emmanuel Arthur[a,*], Hafeez Ur Rehman[a,b], Markus Tuller[c], Nastaran Pouladi[a], Trine Nørgaard[a], Per Moldrup[d], Lis Wollesen de Jonge[a]

[a] Department of Agroecology, Aarhus University, Blichers Allé 20, PO Box 50, DK-8830 Tjele, Denmark
[b] Faculty of Science and Technology, Norwegian University of Life Sciences, Drøbakveien 31, 1430 Ås, Norway
[c] Department of Environmental Science, The University of Arizona, 1177 E. 4th Street, Tucson, AZ 85721, USA
[d] Department of the Built Environment, Aalborg University, Thomas Manns Vej 23, DK-9220, Aalborg, Denmark

ARTICLE INFO

Handling Editor: Yvan Capowiez

Keywords:
Hysteresis
Liquid limit
Plastic limit
Plasticity index
Water sorption isotherms

ABSTRACT

A number of environmental, agronomic and engineering applications require knowledge of the Atterberg limits (liquid limit, LL; plastic limit, PL) and the plasticity index, PI of soils. The tedious and costly nature of standard experimental methods, as well as challenges with measurement repeatability motivated the development of regressions as well as more sophisticated techniques to estimate the Atterberg limits from other properties such as clay content, cation exchange capacity (CEC), and soil specific surface area. The amount of water adsorbed to particle surfaces at relative humidity (RH) < 95% is intimately linked to these soil properties, which suggests that hygroscopic water content (w_h) may be a better predictor of the Atterberg limits. The present study (i) proposes regression models that estimate the LL, PL, and PI from w_h at different relative humidity values ranging from 10 to 90% and considering water sorption hysteresis, and (ii) compares the performance of the models to other models that comprise clay, silt and organic carbon contents and CEC. For model development, w_h was measured by water adsorption and desorption for 168 soil samples that varied widely in terms of geographic origin, clay mineralogy, and soil organic carbon content. The LL and PL were determined with the drop cone penetrometer and rolling device, respectively. Regression models were developed for both sorption directions for nine RH values between 10 and 90%. For 44 independent soil samples, the models estimated LL, PL and PI accurately (e.g., for desorption w_h measured at 90% RH, $RMSE$ and r^2 values were 6.43% & 0.89; 3.95% & 0.83 and 6.69% & 0.79, respectively). There was no clear effect of sorption direction on the estimation accuracy. The w_h determined at higher RH tended to better estimate the Atterberg limits compared to that measured at lower RH. The w_h models were superior in estimating LL and PL compared to models that were based on clay content and organic carbon or CEC. For the PI, the models based on CEC performed slightly better than the w_h models. Thus, a single measure of w_h can provide reliable estimates of the Atterberg limits and PI.

1. Introduction

The Atterberg limits (liquid limit and plastic limit) and the plasticity index of soils, originally proposed by Atterberg (1911), are crucially important for civil engineering, environmental, and agronomic applications. For example, the Atterberg limits serve as the basis for quantifying the swelling and or shrinkage potential of engineering materials (Sivakumar et al., 2009), and in agronomy, the plastic limit (PL) is often used as a measure for the optimum water content for tillage (Keller and Dexter, 2012; Obour et al., 2018). Several methods exist to measure the Atterberg limits, each with their associated merits and demerits. Popular methods for determining the liquid limit (LL) are the classical Casagrande cup method (ASTM, 2017), or the drop cone penetrometer method (BS, 2018). The LL determined by these two methods are often similar for samples with LL < 150% (Kayabali et al., 2016; Rehman et al., 2020; Shimobe and Spagnoli, 2019; Spagnoli, 2012) or can be easily converted from one to the other via a linearity constant (Di Matteo, 2012; Mishra et al., 2012). The PL is traditionally determined with the thread rolling method (ASTM, 2017), which was modified to the rolling device (Bobrowski and Griekspoor, 1992) to eliminate methodological challenges related to the characteristics of the operator's hand among others. Other methodologies for the PL include the Barnes (Barnes, 2009) and the thread bending test (Moreno-Maroto and Alonso-Azcarate, 2015). The commonly used thread rolling and rolling device methods often present similar PL values (Rehman et al., 2020) and may be used interchangeably.

* Corresponding author.
E-mail address: emmanuel.arthur@agro.au.dk (E. Arthur).

https://doi.org/10.1016/j.geoderma.2020.114698
Received 20 May 2020; Received in revised form 21 August 2020; Accepted 29 August 2020
Available online 10 September 2020

All these aforementioned methods for LL and PL are tedious and costly for large sample quantities. Consequently, pedotransfer functions (PTFs) have been developed over the years to estimate LL and PL from easily measurable or readily available soil properties. Soil properties that have been used as predictors of the Atterberg limits include clay, silt, and organic matter contents (de Jong et al., 1990; Gupta et al., 2016; Keller and Dexter, 2012; Stanchi et al., 2017), cation exchange capacity, CEC (Seybold et al., 2008), soil specific surface area, SA (Smith et al., 1985; Yukselen-Aksoy and Kaya, 2010), and soil water content at a matric potential of −1500 kPa (de Jong et al., 1990; Seybold et al., 2008).

Utilizing clay, silt and organic carbon (OC) contents to estimate the Atterberg limits is convenient, as a majority of soil surveys often routinely measure these properties. Unfortunately, the large variations in the expansivity of different clay minerals limits the applicability of any PTF based on clay and silt contents to samples that have similar mineralogy as the samples that were used to develop the PTFs. The CEC and SA of samples are often better estimators of the Atterberg limits, but these are not routinely measured and if the data are unavailable, the cost and time required to measure them are not much different from that required to directly measure the Atterberg limits. Aside the work of de Jong et al. (1990), Seybold et al. (2008), and Smith et al. (1985) where they estimated the Atterberg limits from the water content at −1500 kPa, and hygroscopic water content (w_h), the potential of w_h to estimate the Atterberg limits has received very limited attention.

The w_h is easier to measure, requires minimal laboratory instrumentation (a relative humidity meter, and a regular drying oven), and can be determined for a large number of samples simultaneously. The amount of water adsorbed to soil particle surfaces for relative humidity (RH) < 95% is intimately linked to the clay content, clay mineralogy, silt content (in the case of silt-rich samples), OC content (for samples with large amounts of OC or low clay content) (Arthur et al., 2015), SA (Akin and Likos, 2014; Arthur et al., 2018; Moiseev, 2008), as well as the kind and amount of exchangeable cations (Arthur, 2017; Khorshidi and Lu, 2017). Consequently, w_h or the full water vapor sorption isotherm, has been successfully used to estimate the clay content, SA, and CEC; and these soil properties contribute to the magnitude of the Atterberg limits. Thus, there is a very high potential to use w_h to estimate the Atterberg limits. Based on the above knowledge gaps, we set out to (i) develop a model framework to estimate the Atterberg limits (PL and LL) and PI from hygroscopic water content, considering water sorption hysteresis, and (ii) compared the model performance to direct measurements, PTFs based on CEC, and soil particle size distribution and soil organic carbon.

2. Methodology

2.1. Investigated samples

The samples used for the study comprised 212 soil samples (top soil and sub soil) from 25 countries, with the majority from three continents (Europe 116, Africa 48, and Asia 37) and nine samples from South America and one each from the United States and New Zealand.

2.2. Laboratory measurements

2.2.1. Particle size distribution, and organic carbon content

The particle size distribution of the samples was measured on 2-mm sieved air dry samples with a combination of the wet-sieving and pipette methods after removal of OC and carbonates (when present in a pre-test) (Gee and Or, 2002). Soil organic carbon was determined on ball-milled subsamples by oxidation of carbon at 950 °C with an elemental analyzer.

2.2.2. Atterberg limits

Based on the reported similarity between LL measured with the Casagrande cup and the drop-cone methods for samples with LL < 150% (Shimobe and Spagnoli, 2019), we chose the drop cone method because it is simpler and shows better repeatability (Rehman et al., 2020).

The samples for the determination of the Atterberg limits were sieved to 425 μm prior to the measurements. The LL was determined in triplicate with a semi-automated drop cone penetrometer with a 35 mm long and 30° angle test cone (BS, 2018). In brief, distilled water was added to about 100 g of sample, mixed thoroughly and pushed into the sample cup with a spatula while ensuring that no air was trapped within the sample. The surface of the sample was levelled, and the cone placed so it barely touched the soil surface. The cone was then released automatically for 5 s and the penetration depth recorded. When the penetration depth was less than 12 mm, more water was mixed into the sample until the first reading was around 15 mm. The procedure was repeated three times until the penetration depth ranged between 15 and 25 mm. The gravimetric water content by interpolation that corresponded to a cone penetration depth of 20 mm was taken as the LL.

The PL of the samples was determined in quadruplicate with the device rolling method (ASTM, 2017; Bobrowski and Griekspoor, 1992). About 30 g of sample was mixed with water until it became plastic and easily molded into a ball. The sample was initially rolled by hand into two short threads 5 to 10 mm thick. The soil threads were placed on the bottom plate of the rolling device and the top plate was used to apply a downward force simultaneously with a rolling motion until the top plate touched the 3 mm side rails. The soils were removed and remolded and the procedure repeated until they crumbled. The gravimetric water content of the crumbled samples was considered as the PL.

For both LL and PL measurements, the gravimetric water content of the samples was obtained by oven drying at 105 °C for at least 48 h.

The PI for the samples was calculated as LL – PL.

2.2.3. Hygroscopic water content (w_h)

Water vapor adsorption and desorption isotherms covering the range from 3% ≤ RH ≤ 93% (resolution of 2% RH and measurement temperature of 25 °C) were determined on air dried samples with a vapor sorption analyzer (METER Group Inc., Pullman, WA, USA). After the measurements, the samples were oven dried for 48 h to determine the reference water contents. Full details of the measurement methodology are reported in Arthur et al. (2014) and Likos et al. (2011). For modeling, the water contents at 18 selected RH values (10 to 90% with increments of 5%) were obtained directly from the adsorption and desorption data or by linear interpolation between the two closest points when the w_h at the exact RH was not directly available.

2.3. Modeling

2.3.1. Modeling rationale and data exploration

The use of w_h as a predictor of the Atterberg limits is possible because the limits are controlled primarily by the soil clay mineralogy, surface area and the magnitude of CEC. These soil properties are often used in PTFs to predict the Atterberg limits (e.g., van Tol et al., 2016; Zolfaghari et al., 2015). Hygroscopic water content, is much easier to measure, and its magnitude is determined by a combination of clay content, clay mineralogy, silt content and OC (Karup et al., 2017). Previous work has emphasized the tight link between w_h and both CEC and SA (Arthur et al., 2018; Khorshidi and Lu, 2017). Additionally, a few studies have shown that water content at different RH (or soil water potentials) can be used as predictors for both PL and LL (de Jong et al., 1990; Seybold et al., 2008). It is thus clear that w_h can serve as a reliable estimator of the Atterberg limits.

Prior to the analyses, the relationships between w_h and the LL, PL and PI were explored for all samples. Based on the relationship between w_h and PL, the 212 samples were split into two groups. Group 1 [191 samples] comprised all types of samples, except tropical Vertisols from Ethiopia and Ghana, and Group 2 [21 samples] included the tropical Vertisols.

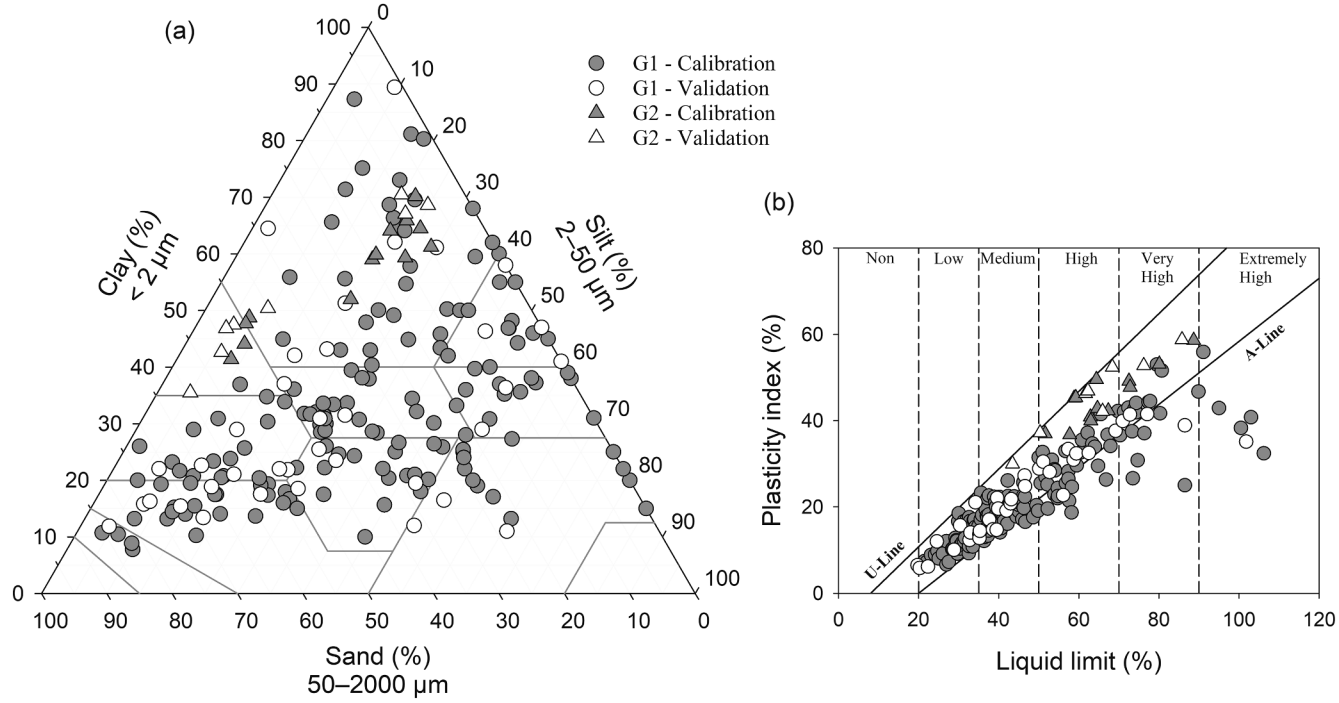

Fig. 1. Distribution of the investigated samples displayed on the (a) USDA soil textural triangle and (b) Casagrande plasticity chart including classification of swelling classes. The samples are partitioned into calibration [grey symbols] and validation [white symbols] datasets for the two sample groups (G1 and G2).

2.3.2. Data partitioning for modeling

The two sample groups were further partitioned into two datasets each; the model development or calibration, and the model validation datasets. The partitioning was done in R v3.5.2 (R Development Core Team, 2018) using the "createDataPartition" data splitting function in the "caret" package (Kuhn, 2019). The function creates balanced splits of the data while preserving their overall class distribution. The samples were split into the two datasets based on LL as it had the largest data range among the three variables. Group 1 (G1) samples were split into 80% [155 samples] and 20% [36 samples] and Group 2 (G2) samples were split as 60% [13 samples] and 40% [8 samples] for the calibration and validation datasets, respectively.

2.3.3. Model development

The suitability of the data for the regression analyses was determined by assessing the normality of the residuals (Shapiro–Wilk test) and constant variance (computing the Spearman rank correlation between the absolute values of the residuals and the observed values) of the data. It was found that the data satisfied both criteria.

2.3.3.1. Hygroscopic water content. For the two calibration datasets, the measured variables (LL, PL, and PI) were regressed individually against the predictor variables (18 w_h values between 10 and 90% *RH* for adsorption and desorption). The analysis was conducted using the lm function in R to fit a linear model to the data.

The general form of the model was:

$$y\% = a + b \times w_h\% \quad (1)$$

where y is LL, PL or PI, w_h is hygroscopic water content at a given relative humidity (*RH*) and a and b are the intercept and slope of the regression model, respectively.

After obtaining the 18 equations each for adsorption and desorption for all three variables (LL, PL, PI), the a-values did not vary significantly with *RH*, so an average a value is provided for each limit. Conversely, b varied markedly with increasing *RH*, so a polynomial function was used to relate the b values to *RH*.

2.3.3.2. PTFs from other soil properties. The calibration datasets were also used to develop other PTFs based on either CEC or a combination of clay, silt and organic carbon contents (denoted as PSD). The CEC PTF was of the same form as for the w_h, whereas the PSD PTF comprising clay, silt and OC was developed using forward stepwise regression, therefore in some cases, not all three variables significantly contributed to the regression and were not included (Table 3). Sand content was excluded as it was collinear with the clay content. Furthermore, as the CEC was strongly correlated to the clay content ($r = 0.71^{***}$) the two variables were not included in the same PTF.

2.4. Evaluation of model performance

The LL, PL, and PI of the samples in the validation datasets was estimated from the models developed from w_h and the other PTFs. The performance of the models was evaluated by the square of the Pearson correlation coefficient, the root mean square error (*RMSE*), and the standardized root mean square error (*sRMSE*) (Equation (2)). The *sRMSE* allows comparison of the model performance to previous studies (Arthur, 2017).

$$RMSE = \sqrt{\sum_{i=1}^{n} \frac{(y_p - y_m)^2}{n}},$$
$$sRMSE = RMSE/Range \quad (2)$$

where n is the number of samples, y_p represents the estimated LL, PL or PI, y_m represents the reference or measured LL, PL or PI, and *Range* is the difference between the smallest and the largest value of the respective variable.

The sensitivity of the w_h models to *RH* was determined by comparing the *RMSE* of the 18 *RH* levels for each sorption direction.

3. Results and discussion

3.1. Description of calibration and validation datasets

The samples exhibited a large variation in Atterberg limits, PI, and other soil properties (Fig. 1, Table 1) and the soil types included

Table 1
Descriptive statistics of soil properties for investigated samples (n = 212).

Property		Min	Max	Mean	CV%
Clay	%w/w	8 [8, 11]	89 [87, 89]	35 [35, 36]	51 [50, 54]
Silt		2 [2, 2]	85 [85, 59]	31 [32, 25]	57 [55, 66]
Sand		0 [0, 0]	85 [85, 84]	34 [32, 39]	70 [72, 61]
OC		0.0 [0.0, 0.0]	4.7 [4.7, 3.4]	1.1 [1.2, 1.0]	95 [97, 86]
LL		20 [22, 20]	106 [106, 102]	49 [49, 50]	37 [37, 38]
PL		12 [12, 13]	74 [74, 67]	25 [25, 23]	39 [38, 42]
PI		6 [7, 6]	59 [59, 59]	25 [24, 27]	50 [50, 51]
CEC	$cmol_{(+)}\ kg^{-1}$	3 [3, 5]	87 [87, 79]	28 [27, 30]	67 [66, 70]

CV = coefficient of variation; OC = soil organic carbon; LL = liquid limit; PL = plastic limit; PI= plasticity index; CEC = cation exchange capacity. For each soil property, numbers outside square brackets are for the full dataset and the numbers in square brackets are for the calibration and validation datasets, respectively.

Andisols, Luvisols, Oxisols, Vertisols, Chernozems, among others.

The particle size distributions of the investigated samples covered all USDA soil textural classes, except silt (Fig. 1a). The OC and CEC ranged from 0 to 4.7% w/w and 3 to 87 $cmol_{(+)}\ kg^{-1}$, respectively (Table 1). Similarly, the Atterberg limits covered a wide range for the samples; LL from 20 to 106%; PL from 12 to 74%, and the PI from 6 to 59%. Due to the wide variation in LL, the samples covered a broad range in swelling potential (low to extremely high) (Fig. 1b). This wide range in swelling potential of the samples is necessary to ensure broad applicability of the developed models. The partitioning of the dataset into the calibration and validation datasets yielded evenly distributed groups (Fig. 1), considering both the Atterberg limits on the one hand, and soil properties (clay, silt, sand, OC, and CEC) on the other hand (Table 1).

3.2. Relationship between Atterberg limits and w_h

Examples of measured water vapor sorption isotherms for two samples that differ significantly in clay content and plasticity are shown in Fig. 2a. The sample with LL of 54% had significantly higher water sorption than the sample with 27% LL. For both samples, water sorption hysteresis was evident. Hysteresis of water vapor sorption occurs in the majority of soil types; larger hysteresis occurs in soil samples rich in expansive clays such as montmorillonite and limited hysteresis in samples rich in kaolinite (Arthur et al., 2020). The majority of investigated samples considered in this study had varying amounts of swelling clays and only a few samples (< 10 samples) had significantly large amounts of kaolinites or other non-expansive clays in their clay fraction. An example of how w_h at *RH* of 50% (w_{h50d}) was obtained for both adsorption and desorption is shown in Fig. 2a; for the sample with high LL, the w_h at 50% *RH* was 3.01 and 3.65% during adsorption and desorption, respectively. This further justified the need for separate estimation models for adsorption and desorption.

In Fig. 2b and 2c, the relationship between the LL and w_{h50d}, and PL and w_{Ds50}, respectively, are presented. The relationship between PI and w_{Ds50} was similar to that of LL and w_{Ds50} (data not shown). The PL and LL increased linearly as w_h increased. Based on the PL–w_{Ds50} relationship, the samples from G2 were distinctly different from the rest of the samples (Fig. 2c).

The G2 samples were tropical Vertisols with high plasticity due to comparatively low PL relative to LL (Fig. 1b). The high plasticity of Vertisols is due to the strong expansivity of the montmorillonite clay minerals present (Woldeab, 1988). The trends presented for w_{Ds50} and the Atterberg limits (Fig. 2b and 2c) were similar for all considered *RH* levels. Besides a few studies (de Jong et al., 1990; Seybold et al., 2008; Smith et al., 1985), the potential of using water content as an estimator for the Atterberg limits has not been widely investigated. The work of Smith et al. (1985) considering 66 samples from 32 sites in Israel, showed that w_h (*RH* undefined) better explained the variations in LL and PL, when compared to clay content, CEC or SA. In Seybold et al. (2008), based on samples from all over the U.S., the water content at −1500 kPa (w_{1500}), in combination with OC, was used to estimate LL and PL of Andisols, but w_{1500} was only considered because for Andisols, accurate determination of clay content, which was the main predictor for LL and PL, was challenging. In addition to the water content at −1500 kPa, de Jong et al. (1990) found, based on 448 samples from southern Saskatchewan, Canada, that the water content at −33 kPa was better correlated to the Atterberg limits than other soil properties (clay, OC and inorganic C). Beside the Atterberg limits, Lu and Dong (2017) also reported that the maximum adsorption water content was strongly correlated (r = 0.89) to the shrinkage rate for seven samples. Based on the data from Fig. 2 and the literature, it is evident that the soil consistency limits are correlated to w_h.

3.3. Regression models

3.3.1. Hygroscopic water content considering hysteresis

The developed models for the Atterberg limits based on w_h at selected *RH* values between 10 and 90% obtained via adsorption or desorption, are presented in Tables S1 and S2 for the G1 and G2 samples, respectively. For all models, the strength of the relationship between the Atterberg limits and w_h (r^2) exhibited in the regression models tended to increase as *RH* increased from 10 to 90% (Tables S1 and S2).

For G1 samples, the average coefficient of determination (r^2) for the Atterberg limits regression models based on w_h decreased in the order LL (0.76) > PL (0.69) > PI (0.51). Thus, w_h accounted for the variability in LL more than the variability in PL or PI of the investigated samples. Similarly, Smith et al. (1985) reported stronger correlations between w_h and LL (r^2 = 0.72), compared to w_h and PL (r^2 = 0.67). The case was different for the G2 samples, where the relationship between w_h and PL (r^2 = 0.88) was stronger than between w_h and LL (r^2 = 0.74) or PI (r^2 = 32). The highly plastic nature of the Vertisols in G2 suggest that the PL, rather than the LL, may be more strongly linked to the montmorillonite-dominated mineralogy, and consequently w_h.

For each model, the intercept *a* did not vary significantly with *RH*, as observed from the low standard error values of < 1% (Table 2). The average *a* values for the *RH* range are reported in Table 2 for both sample groups and sorption direction. The *a* values for the G1 samples averaged approximately 26, 14, and 12% for LL, PL and PI, respectively, and were not significantly affected by sorption hysteresis. Conversely, for the G2 samples, *a* values for adsorption and desorption were noticeably different (e.g., 16.8 and 20.5% for LL). This may be explained by the larger hysteresis that is observed for samples rich in montmorillonite clay compared to other samples (Arthur et al., 2020). On the other hand, the slope *b* values changed markedly with *RH*, and the generated *b*-*RH* polynomial relationships are presented in Table 2. An example of the fit of the polynomial function to the *b*-*RH* data is presented in Fig. 3 for the LL of the G1 samples. The polynomial function accurately fitted the *b*-*RH* data for all sample groups and for both sorption directions. For all the Atterberg limits, sorption directions and two sample groups, the polynomial function fits to the *b*-*RH* data

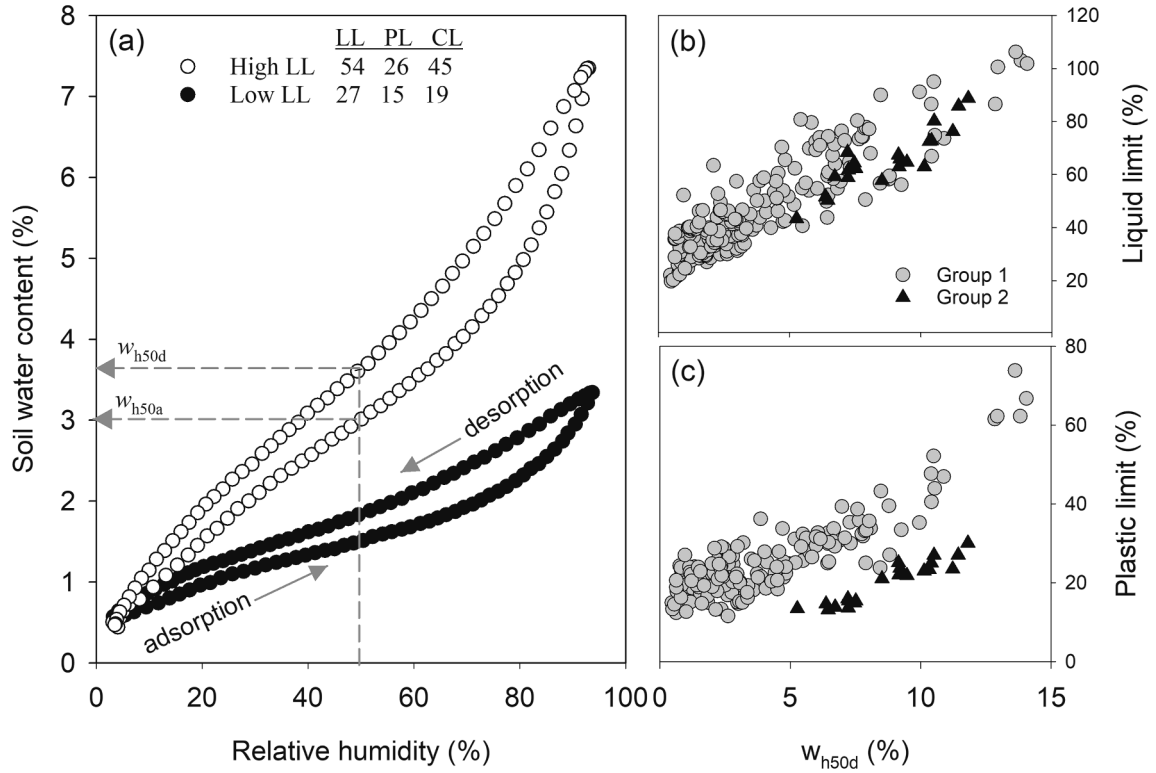

Fig. 2. (a) Soil water vapor sorption isotherms for two samples with different clay content (CL) and Atterberg limits, depicting adsorption and desorption, hysteresis and derivation of the hygroscopic water contents (w_h) at relative humidity (RH) of 50% (w_{h50d}), and the relationship between w_{h50d} and (b) liquid limit, and (c) plastic limit for the two soil sample groups.

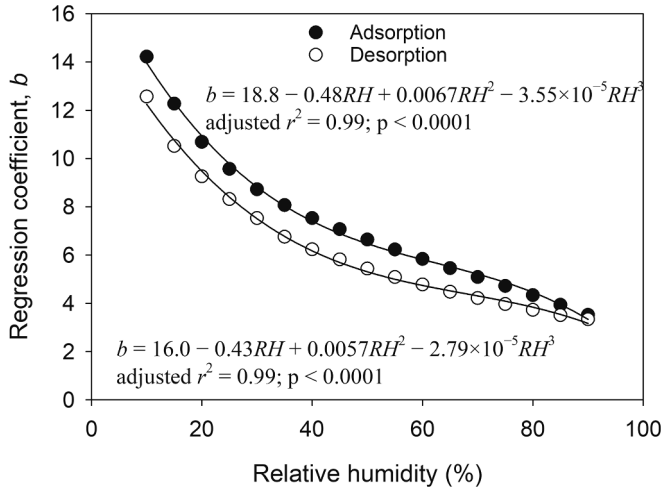

Fig. 3. Relation between relative humidity and water content coefficient, *b*, of the proposed equation for estimating the liquid limit (LL% = $a + b \times w_h$%) for Group 1 samples. The intercept, *a*, averaged 26.62 and 26.11% for water vapor adsorption and desorption, respectively. The average *a* values and polynomial functions for estimating plastic limit and the plasticity index are provided in Table 2.

had r^2 values between 0.966 and 0.998 and residual standard error values between 0.058 and 0.193 (Table 2).

3.3.2. PTFs based on other soil properties

The use of soil texture, OC, CEC, and other soil properties to estimate the Atterberg limits using regression analyses has been exploited in several studies with varying degrees ($0.47 < r^2 < 0.87$) of success (e.g., Ahmadi et al., 2012; Seybold et al., 2008; Spagnoli and Shimobe, 2019; van Tol et al., 2016). In Table 3, the regression coefficients for the PTFs based on clay, silt and OC content (denoted as PSD), and based on CEC are presented. Although sand content is sometimes used as an estimator variable for the Atterberg limits (Deng et al., 2017; Keller and Dexter, 2012), it was excluded from the analyses because the amount of water sorbed by sand particles is negligible and the sand content of the datasets was collinear with the clay content. Clay content was a significant ($p < 0.001$) predictor variable for PL, LL and PI for both sample groups. In general, higher clay content is linked to higher plasticity and shrink-swell potential in soils. Also, silt content was an important variable to estimate the LL and PI for both sample groups, but less so for the PL. Although the majority of existing PTFs do not include silt in regression models, the fine silt fraction can reportedly absorb substantial amounts of water during the soil wetting process (Karup et al., 2017). Organic carbon content did not significantly contribute to all the Atterberg limits for G2 samples, while for G1 samples, OC had no significant contribution to PL. This can be partly explained by the low average OC (1.1%) of the entire dataset (Table 1). For samples with substantial amounts of OC, previous studies have indicated a strong correlation between OC and the PL (de Jong et al., 1990; Keller and Dexter, 2012; Mbagwu and Abeh, 1998). For example, Keller and Dexter (2012) reported that for samples with similar soil texture, OC strongly affected the PL. Also, de Jong et al. (1990) showed that OC was equally important as clay content in estimating LL of samples from Ap horizons. Conversely, Seybold et al. (2008) found no significant correlation between OC and the Atterberg limits (LL and PI).

Additionally, for soil samples with clay contents > 20% and OC < 2.0%, the contribution of OC to water content is reportedly insignificant relative to that of clay content (Arthur et al., 2015). Since the average clay content of the investigated samples was 35%, this may also explain the limited effect of OC on the Atterberg limits for the G1 samples. For some of the PSD models for the G2 samples, the intercepts were not significant and were removed from the equation; this implies that the r^2 values of these equations cannot be compared to the other

Table 2
Parameters of the Atterberg limits (liquid limit, LL and plastic limit, PL) and the plasticity index (PI) regression models (y% = $a + b \times w_h$%) from hygroscopic water content, w_h, considering hysteresis for Group 1 and Group 2 samples. a and b values for each relative humidity are provided in Tables S1 and S2.

Property (%)	S_d	a	b			
			Equation	adj. r^2	p-value	RSE
Group 1 samples						
LL	Ads	26.6 ± 0.35	$18.8–0.48x + 0.0067x^2 - 3.55 \times 10^{-5}x^3$	0.997	< 0.0001	0.167
	Des	26.1 ± 0.32	$16.0–0.43x + 0.0057x^2 - 2.79 \times 10^{-5}x^3$	0.996	< 0.0001	0.159
PL	Ads	14.5 ± 0.19	$9.19–0.25x + 0.0035x^2 - 1.90 \times 10^{-5}x^3$	0.997	< 0.0001	0.085
	Des	14.2 ± 0.17	$8.08–0.21x + 0.0029x^2 - 1.42 \times 10^{-5}x^3$	0.995	< 0.0001	0.094
PI	Ads	12.1 ± 0.16	$8.92–0.23x + 0.0032x^2 - 1.65 \times 10^{-5}x^3$	0.997	< 0.0001	0.082
	Des	11.9 ± 0.16	$7.91–0.21x + 0.0028x^2 - 1.37 \times 10^{-5}x^3$	0.997	< 0.0001	0.067
Group 2 samples						
LL	Ads	16.8 ± 0.46	$23.1–1.02x + 0.024x^2 - 2.64 \times 10^{-4}x^3 + 1.05 \times 10^{-6}x^4$	0.998	< 0.0001	0.135
	Des	20.5 ± 0.72	$13.3 - 0.33x + 0.0044x^2 - 2.17 \times 10^{-5}x^3$	0.991	< 0.0001	0.193
PL	Ads	−7.0 ± 0.21	$12.8–0.51x + 0.013x^2 - 1.16 \times 10^{-4}x^3 + 4.31 \times 10^{-7}x^4$	0.998	< 0.0001	0.084
	Des	−6.2 ± 0.24	$8.38 - 0.22x + 0.0031x^2 - 1.54 \times 10^{-5}x^3$	0.998	< 0.0001	0.054
PI	Ads	23.8 ± 0.32	$10.5–0.50x + 0.013x^2 - 1.48 \times 10^{-4}x^3 + 6.21 \times 10^{-7}x^4$	0.998	< 0.0001	0.058
	Des	26.7 ± 0.54	$5.07 - 0.13x + 0.0019x^2 - 9.99 \times 10^{-6}x^3$	0.966	< 0.0001	0.134

S_d = sorption direction, Ads = adsorption, Des = desorption, x = relative humidity (%) between 10 and 90%, RSE = residual standard error of regression, adj. r^2 = adjusted r-squared of regression; p-value = significance of the regression. All regression coefficients were significant at the 0.001 level.

equations that include intercepts.

The CEC tended to more strongly relate to the Atterberg limits than the clay, silt and OC contents; as CEC integrates the three soil properties in addition to the clay mineralogy to estimate the Atterberg limits. Based on different types and number of soil samples, Seybold et al. (2008) and Smith et al. (1985) also reported similar strong correlations between CEC and the Atterberg limits.

3.4. Validation of developed models

3.4.1. Hygroscopic water content models

The performance of the developed models was evaluated for all 44 validation samples together (36 and 8 for G1 and G2, respectively). The validation dataset comprised of samples from 14 countries that varied widely in clay mineralogy (kaolinite, illite, and montmorillonite clay minerals) and the magnitude of the estimated parameters (LL, PL and PI). Further details of each sample in the validation set is provided in Table S1. The validation was done by (i) scatterplots of the measured and estimated Atterberg limits (Fig. 4 and Fig. 5), and (ii) comparison of the estimated swelling classes based on the LL and PI (Fig. 1b; Table 4).

A comparison of the measured and estimated Atterberg limits from desorption w_h measured at *RH* of 50 and 90%, respectively, is presented in Fig. 4 and for all *RH* levels and sorption directions in Fig. S1. In general, there was slightly better estimation of Atterberg limits based on the w_h at 90% *RH* compared to 50% *RH* (Fig. 4). When the whole *RH* range is considered, the trend is clearer; the estimation accuracy for LL and PL increases (decreasing *RMSE*) with increasing *RH* (Fig. S1). The discontinuity in the trend for PI in Fig. S1 is possibly an artefact from combining the two sample groups.

For different sorption directions, the average *RMSE* (%) over the entire *RH* range from 10 to 90% for adsorption (LL = 7.73%; PL = 4.58%, and PI = 6.68%) was slightly larger than for desorption (LL = 7.39%; PL = 4.35%, and PI = 6.65%), and beside the PI, the desorption-based estimations were always better than for adsorption (Fig. S1). The seemingly better estimation of Atterberg limits based on desorption water content, is possibly due to the greater intermolecular forces the adsorption process has to overcome compared to desorption. Previous studies also suggest to use desorption data for estimating soil properties (Arthur, 2017; Lu and Khorshidi, 2015). The performance of the models was in the order LL > PL > PI (e.g., estimation based w_h at 90% *RH* gave r^2 values of 0.89, 0.83 and 0.79, respectively for LL, PL and PI).

3.4.2. CEC and PSD models

The performance of the CEC- and PSD-based models for estimating the Atterberg limits is shown in Fig. 5. Results indicate that CEC was better at estimating the Atterberg limits compared to the PSD. Both

Table 3
Regression coefficients for pedotransfer functions based on clay, silt and organic carbon contents (PSD) and based on cation exchange capacity (CEC) for Group 1 and Group 2 samples.

	LL		PL		PI	
	Group 1	Group 2	Group 1	Group 2	Group 1	Group 2
Partial regression coefficients - Model 1 (PSD)						
Intercept	16.5^{***}	–	12.2^{***}	–	5.6^{**}	–
Clay [%]	0.82^{***}	1.40^{***}	0.39^{***}	0.27^{***}	0.44^{***}	1.12^{***}
Silt [%]	0.18^{***}	0.70*	–	0.30*	0.13^{***}	-1.00^{***}
OC [%]	-2.29^{**}	–	–	–	-1.84^{***}	–
Adj. r^2	0.66	0.99	0.46	0.99	0.57	0.99
RSE	10.44	4.84	7.10	1.95	7.02	4.00
Partial regression coefficients - Model 2 (CEC)						
Intercept	23.9^{***}	25.8^{**}	13.6^{***}	–	10.3^{***}	20.9^{**}
CEC [$cmol_{(+)}\ kg^{-1}$]	0.95^{***}	0.73^{***}	0.47^{***}	0.37^{***}	0.48^{***}	0.44^{***}
Adj. r^2	0.77	0.73	0.62	0.96	0.56	0.64
RSE	8.16	5.19	5.73	4.23	6.32	3.79

***, **, and * denote statistical significance of the regression parameters at $p < 0.001$, 0.01 and 0.05, respectively.
OC = organic carbon, RSE = residual standard error of regression, adj. r^2 = adjusted r-squared of regression.

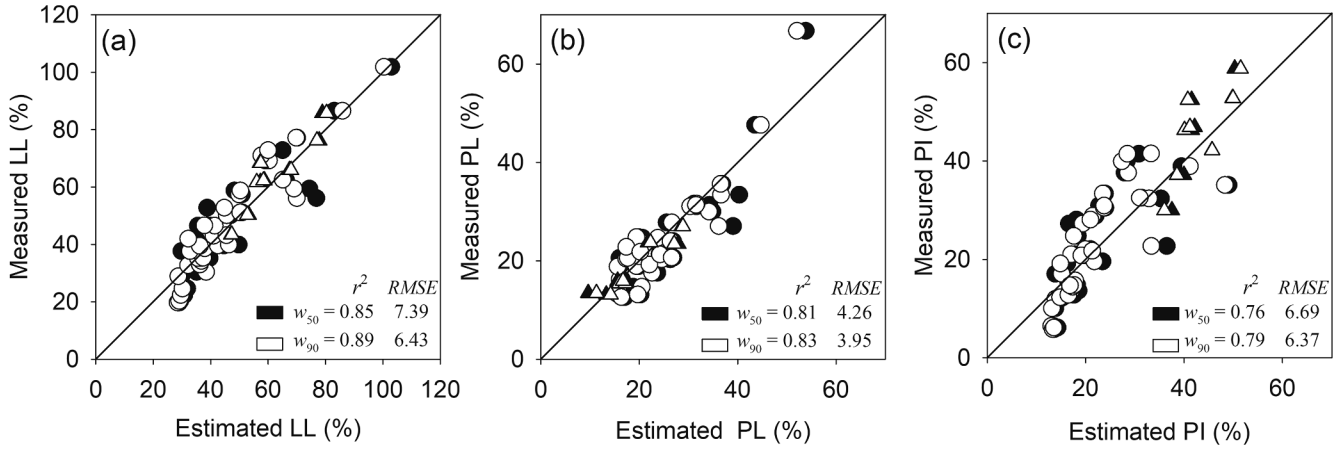

Fig. 4. Measured versus estimated (a) liquid limit, (b) plastic limit, and (c) plasticity index from desorption water content at 50% [w_{50}] and at 90% relative humidity [w_{90}] for Group 1 (○) and Group 2 (Δ) samples. RMSE = root mean square error; r^2 = square of the Pearson correlation coefficient.

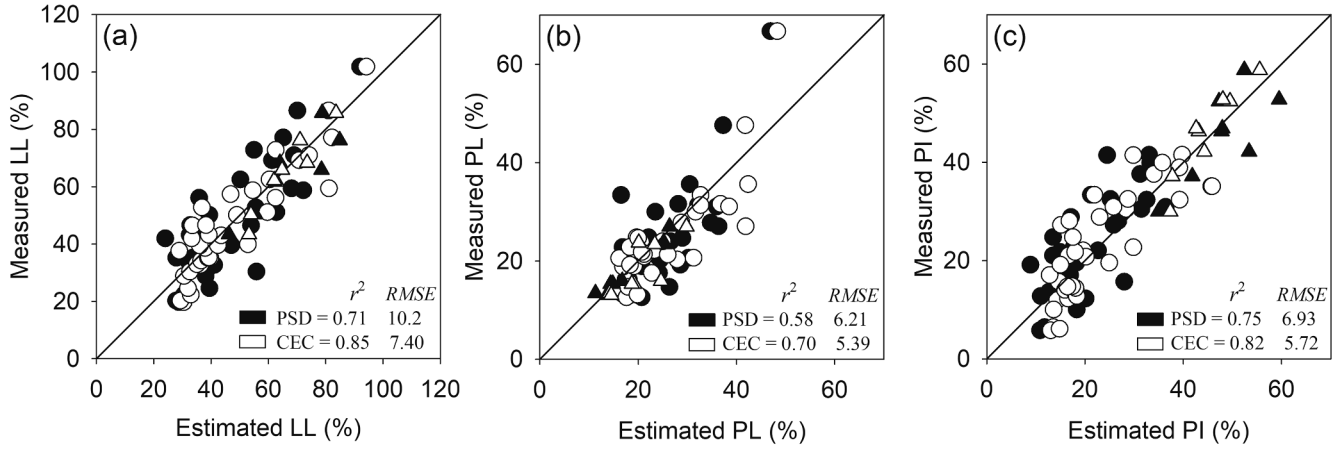

Fig. 5. Measured versus estimated liquid limit (a), plastic limit (b), and plasticity index (c) from clay, silt and organic carbon contents [PSD] and cation exchange capacity [CEC] for Group 1 (○) and Group 2 (Δ) samples. *RMSE* = root mean square error; r^2 = square of the Pearson correlation coefficient.

Table 4
Comparison of percentage of samples classified into the correct swelling class after estimation of liquid limit using desorption water content at 90%*RH* (w_{h90d}), cation exchange capacity (CEC), or a combination of clay, silt and organic carbon contents (PSD).

Swelling class based on LL (Fig. 1)	Percent correctly classified		
	w_{h90d}	CEC	PSD
Low [9]	78	78	44
Medium [14]	93	64	43
High [16]	81	75	75
Very high [4]	100	75	50
Extremely high [1]	100	100	100

models exhibited Atterberg limits estimation values that were evenly distributed along the 1:1 line with no clear underestimations or overestimations.

3.5. Comparison of newly developed models

Comparison of the w_h-based models (Fig. 4) and the models based on CEC and PSD (Fig. 5) showed that for the LL and PL, the model based on w_h was superior to the other two models. For the PI, however, the difference among the three developed models was minimal; but the CEC based model tended to better estimate PI when compared to the w_h and PSD models.

How this translates to the classification of the samples into swelling classes for engineering purposes is shown in Table 4. The data in the table describe the percentage of samples that were classified into the same swelling class based on the model estimations compared to the measured LL data (see Fig. 1b for swelling class classification).

For the samples with low swelling potential, w_h and CEC correctly classified 78% compared to the just 44% by the PSD-based model. For the samples with medium and high swelling potential, w_h classified 93% and 81%, respectively; better than using CEC and PSD. Additionally, CEC and w_h were both good at correctly classifying the five samples with very high and extremely high swelling potential. Overall, this was also consistent with what was observed earlier in Figs. 4 and 5, that among the three model types, the PSD had the highest estimation error. Nevertheless, the estimation accuracy of PSD will be sufficient for the purpose of screening samples into plasticity or swelling groups. Additionally, since w_h data are not readily available at regional or country scale, the CEC and PSD models may be more convenient to use as the data is often readily available from standard soil surveys.

3.6. Evaluation of models from literature

Existing PTFs from three studies were evaluated and their performance compared with the models developed in this study. Firstly, de Jong et al. (1990), based on 279 samples from Saskatchewan, Canada, used stepwise multiple linear regression to develop equations for the

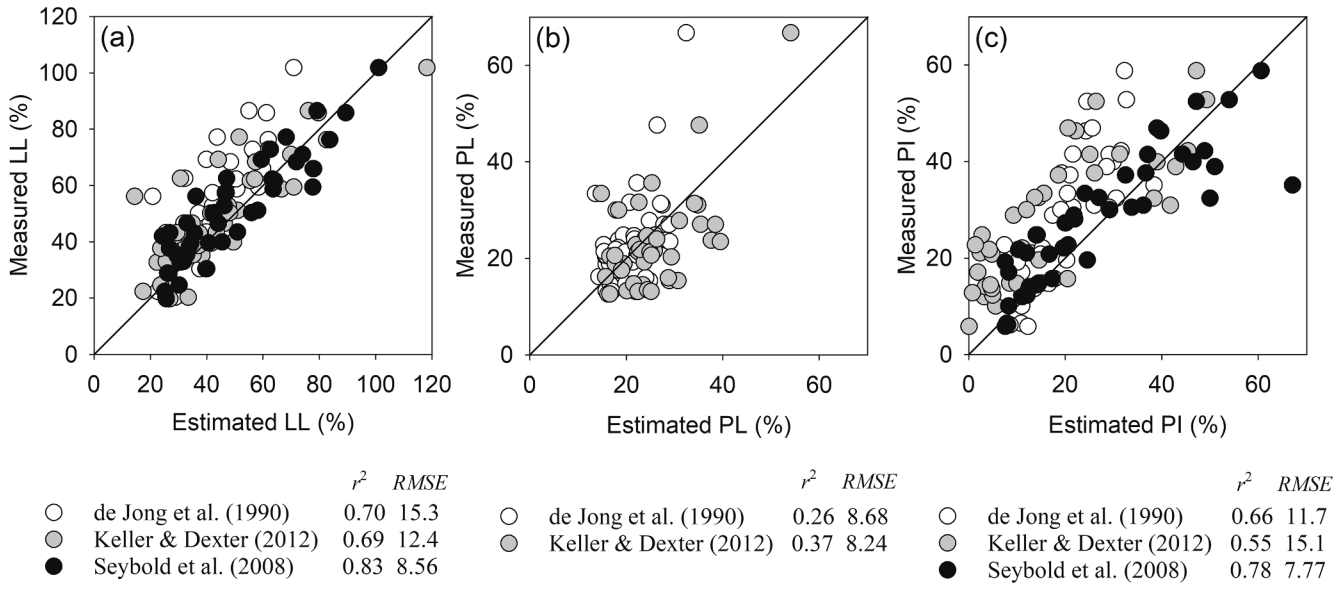

Fig. 6. Comparison of the performance of pedotransfer functions from literature for estimating the (a) liquid limit [LL], (b) plastic limit [PL], and (c) plasticity index [PI] from clay content, organic carbon and cation exchange capacity. See Table S4 for the pedotransfer functions. RMSE = root mean square error; r^2 = square of the Pearson correlation coefficient.

LL, PL and PI from clay and OC contents. Secondly, Keller and Dexter (2012) used 89 samples from nine countries to develop equations, from clay and organic matter contents, for PL, LL and PI. Finally, Seybold et al. (2008) utilized a database of 2797 samples from all over the USA, and developed predictive equations for the LL and PI by combining clay content and CEC. All the equations are provided in Table S4.

In Fig. 6, the performance of the three groups of models are presented for the validation dataset (both G1 and G2 samples). The three considered models estimated the Atterberg limits with varying degrees of accuracy. For LL, the Seybold et al. (2008) model performed best (*RMSE* = 8.56%) among the three studies, while the model of de Jong et al. (1990) had the highest estimation error (*RMSE* = 15.3%) (Fig. 6a). For PL, the performance of the two evaluated models was significantly poorer than for LL (Fig. 6b). For PI, the performance of the Keller and Dexter (2012) model was the lowest among the three (*RMSE* = 15.11%), while the Seybold et al. (2008) model performed creditably well (*RMSE* = 7.77%). The better performance of the Seybold et al. (2008) model is due to the inclusion of CEC, which as mentioned earlier is a more representative variable for available surfaces for water absorption. The use of clay and OC or OM contents alone do not account for the significant contribution of clay mineralogy in determining the magnitude of the Atterberg limits.

The three literature models estimated the LL, PL, and PI with a lower accuracy (Fig. 6) than the models based on the w_h (Fig. 4), primarily because w_h better explains the variability in the Atterberg limits and PI, compared to soil texture or OC. Although the CEC and PSD models presented here used the same soil properties as used in the models from literature, the performance of the proposed models (Fig. 5) were better than the models from literature. This is due to the large variability in the samples used for developing the models in our study.

3.7. Model limitations

The maximum LL, PL and PI of the samples considered in the study were 106, 74, and 59%, respectively. Consequently, the models developed may not be applicable for high plastic samples (LL > 110%) or to samples of very low plasticity (PI < 10%). Further, the investigated samples did not contain large amounts of salts, so the applicability of the models for saline, sodic or gypsic samples may be limited.

4. Conclusion

We propose regression models that estimate the Atterberg limits and the plasticity index (PI) from hygroscopic water content (w_h) measured between 10 and 90% relative humidity (*RH*) and considering hysteresis. Furthermore, we compared w_h models with models based on cation exchange capacity (CEC), clay, silt, and organic carbon contents. The w_h–based models accurately predicted liquid limit (LL) and plastic limit (PL) regardless of the *RH* at which w_h is measured or the sorption direction for a wide range of soil types. Furthermore, the w_h–based models for LL and PL were superior to models developed in the study or from the literature that were based on other soil properties. For PI, although the w_h–based models performed creditably well, other models that incorporated CEC performed slightly better. Thus, for studies that require the Atterberg limits on a large scale with no available soil data, the w_h–based models will prove useful as they require only a *RH* meter and a drying oven.

Declaration of Competing Interest

The authors declare that they have no known competing financial interests or personal relationships that could have appeared to influence the work reported in this paper.

Acknowledgements

This research was financed by VILLUM FONDEN research grant 13162. We especially thank the numerous researchers who generously provided samples for the work.

Appendix A. Supplementary data

Supplementary data to this article can be found online at https://doi.org/10.1016/j.geoderma.2020.114698.

References

Ahmadi, A.A., Talaie, B.E., Soukoti, C.R., 2012. Pedotransfer functions for estimating Atterberg limits in semi-arid areas. Int. J. Agric.: Res. Rev. 2 (4), 491–495.
Akin, I.D., Likos, W.J., 2014. Specific surface area of clay using water vapor and EGME sorption methods. Geotech. Test. J. 37 (6), 1016–1027.

Arthur, E., 2017. Rapid estimation of cation exchange capacity from soil water content. Eur. J. Soil Sci. 68 (3), 365–373.
Arthur, E., Tuller, M., Moldrup, P., de Jonge, L.W., 2014. Evaluation of a fully automated analyzer for rapid measurement of water vapor sorption isotherms for applications in soil science. Soil Sci. Soc. Am. J. 78 (3), 754–760.
Arthur, E., Tuller, M., Moldrup, P., de Jonge, L.W., 2020. Clay content and mineralogy, organic carbon and cation exchange capacity affect water vapour sorption hysteresis of soil. Eur. J. Soil Sci. 71 (2), 204–214.
Arthur, E., Tuller, M., Moldrup, P., Greve, M.H., Knadel, M., de Jonge, L.W., 2018. Applicability of the Guggenheim–Anderson–Boer water vapour sorption model for estimation of soil specific surface area. Eur. J. Soil Sci. 69 (2), 245–255.
Arthur, E., Tuller, M., Moldrup, P., Jensen, D.K., de Jonge, L.W., 2015. Prediction of clay content from water vapour sorption isotherms considering hysteresis and soil organic matter content. Eur. J. Soil Sci. 66 (1), 206–217.
ASTM, 2017. ASTM D4318-17e1, Standard test methods for liquid limit, plastic limit, and plasticity index of soils. ASTM International, 2017, West Conshohocken, PA.
Atterberg, A., 1911. Über die physikalische Bodenuntersuchung und über die Plastizität der Tone. Internationale Mitteilungen für Bodenkunde 1, 10–43.
Barnes, G.E., 2009. An apparatus for the plastic limit and workability of soils. P I Civil Eng.-Geotec. 162 (3), 175–185.
Bobrowski, L., Griekspoor, D., 1992. Determination of the plastic limit of a soil by means of a rolling device. Geotech. Test. J. 15, 284–287.
BS, 2018. Geotechnical investigation and testing – Laboratory testing of soil. BS EN ISO 17892-12:2018, Part 12: Determination of liquid and plastic limits. International Organisation for Standardization, Switzerland.
de Jong, E., Acton, D.F., Stonehouse, H.B., 1990. Estimating the Atterberg limits of Southern Saskatchewan soils from texture and carbon contents. Can. J. Soil Sci. 70 (4), 543–554.
Deng, Y.S., Cai, C.F., Xia, D., Ding, S.W., Chen, J.Z., Wang, T.W., 2017. Soil Atterberg limits of different weathering profiles of the collapsing gullies in the hilly granitic region of southern China. Solid Earth 8 (2), 499–513.
Di Matteo, L., 2012. Liquid limit of low- to medium-plasticity soils: comparison between Casagrande cup and cone penetrometer test. B. Eng. Geol. Environ. 71 (1), 79–85.
Gee, G.W., Or, D., 2002. Particle-size analysis. In: J.H. Dane, G.C. Topp (Eds.), Methods of soil analysis. Part 4. SSSA Book Series No. 5. SSSA, Madison, WI, pp. 255-293.
Gupta, A., Das, B.S., Kumar, A., Chakraborty, P., Mohanty, B., 2016. Rapid and Noninvasive Assessment of Atterberg Limits Using Diffuse Reflectance Spectroscopy. Soil Sci. Soc. Am. J. 80 (5), 1283–1295.
Karup, D., Moldrup, P., Tuller, M., Arthur, E., de Jonge, L.W., 2017. Prediction of the soil water retention curve for structured soil from saturation to oven-dryness. Eur. J. Soil Sci. 68 (1), 57–65.
Kayabali, K., Akturk, O., Fener, M., Ozkeser, A., Ustun, A.B., Dikmen, O., Harputlugil, F., Asadi, R., 2016. Determination of Atterberg limits using newly devised mud press machine. J. Afr. Earth Sc. 116, 127–133.
Keller, T., Dexter, A.R., 2012. Plastic limits of agricultural soils as functions of soil texture and organic matter content. Soil Res. 50 (1), 7–17.
Khorshidi, M., Lu, N., 2017. Determination of cation exchange capacity from soil water retention curve. J. Eng. Mech. 143 (6).
Kuhn, M., 2019. caret: Classification and Regression Training. R package version 6.0-84. https://CRAN.R-project.org/package=caret.
Likos, W.J., Lu, N., Wenszel, W., 2011. Performance of a dynamic dew point method for moisture isotherms of clays. Geotech. Test. J. 34 (4), 373–382.
Lu, N., Dong, Y., 2017. Correlation between soil-shrinkage curve and water-retention characteristics. J. Geotech. Geoenviron. 143 (9).
Lu, N., Khorshidi, M., 2015. Mechanisms for soil-water retention and hysteresis at high suction range. J. Geotech. Geoenviron. 141 (8), 04015032.
Mbagwu, J.S.C., Abeh, O.G., 1998. Prediction of engineering properties of tropical soils using intrinsic pedological parameters. Soil Sci. 163 (2), 93–102.
Mishra, A.K., Ohtsubo, M., Li, L.Y., Higashi, T., 2012. Influence of various factors on the difference in the liquid limit values determined by Casagrande's and fall cone method. Environ. Earth Sci. 65 (1), 21–27.
Moiseev, K.G., 2008. Determination of the specific soil surface area from the hygroscopic water content. Eurasian Soil Sci.+ 41 (7), 744–748.
Moreno-Maroto, J.M., Alonso-Azcarate, J., 2015. An accurate, quick and simple method to determine the plastic limit and consistency changes in all types of clay and soil: The thread bending test. Appl. Clay Sci. 114, 497–508.
Obour, P.B., Jensen, J.L., Lamande, M., Watts, C.W., Munkholm, L.J., 2018. Soil organic matter widens the range of water contents for tillage. Soil Till Res. 182, 57–65.
R Development Core Team, 2018. R: A language and environment for statistical computing. R Foundation for Statistical Computing, Vienna, Austria, URL http://www.R-project.org/.
Rehman, H.U., Pouladi, N., Pulido-Moncada, M., Arthur, E., 2020. Repeatability and agreement between methods for determining the Atterberg limits of fine-grained soils. Soil Sci. Soc. Am. J. https://doi.org/10.1002/saj2.20001(n/a).
Seybold, C.A., Elrashidi, M.A., Engel, R.J., 2008. Linear regression models to estimate soil liquid limit and plasticity index from basic soil properties. Soil Sci. 173 (1), 25–34.
Shimobe, S., Spagnoli, G., 2019. A global database considering Atterberg limits with the Casagrande and fall-cone tests. Eng. Geol. 260, 105201.
Sivakumar, V., Glynn, D., Cairns, P., Black, J.A., 2009. A new method of measuring plastic limit of fine materials. Geotechnique 59 (10), 813–823.
Smith, C.W., Hadas, A., Dan, J., Koyumdjisky, H., 1985. Shrinkage and Atterberg limits in relation to other properties of principal soil types in Israel. Geoderma 35 (1), 47–65.
Spagnoli, G., 2012. Comparison between Casagrande and drop-cone methods to calculate liquid limit for pure clay. Can. J. Soil Sci. 92 (6), 859–864.
Spagnoli, G., Shimobe, S., 2019. A statistical reappraisal of the relationship between liquid limit and specific surface area, cation exchange capacity and activity of clays. J. Rock Mech. Geotech. 11 (4), 874–881.
Stanchi, S., Catoni, M., D'Amico, M.E., Falsone, G., Bonifacio, E., 2017. Liquid and plastic limits of clayey, organic C-rich mountain soils: Role of organic matter and mineralogy. Catena 151, 238–246.
van Tol, J.J., Dzene, A.R., Le Roux, P.A.L., Schall, R., 2016. Pedotransfer functions to predict Atterberg limits for South African soils using measured and morphological properties. Soil Use Manag. 32 (4), 635–643.
Woldeab, A., 1988. Physical properties of Ethiopian Vertisols. In: Jutzi, S.C., Hanque, I., Stares, J.E.S. (Eds.), Management of Vertisols in sub-saharan Africa. ILCA, ILCA, Addis Abba, Ethiopia.
Yukselen-Aksoy, Y., Kaya, A., 2010. Method dependency of relationships between specific surface area and soil physicochemical properties. Appl. Clay Sci. 50 (2), 182–190.
Zolfaghari, Z., Mosaddeghi, M.R., Ayoubi, S., 2015. ANN-based pedotransfer and soil spatial prediction functions for predicting Atterberg consistency limits and indices from easily available properties at the watershed scale in western Iran. Soil Use Manag. 31 (1), 142–154.